

# THE STRUCTURE AND MECHANICAL PROPERTIES OF ALUMINA FILM PREPARED BY RF DIODE SPUTTERING

<sup>1</sup>H. Panitchakan and <sup>2</sup>P. Limsuwan

<sup>1</sup>Department of Physics, King Mongkut's University of Technology Thonburi, Bangkok 10140, Thailand

<sup>2</sup>Thailand Center of Excellence in Physics, CHE, Ministry of Education, Bangkok 10400, Thailand

Received 2013-04-29; Revised 2013-04-29; Accepted 2013-07-17

## ABSTRACT

Alumina ( $\text{Al}_2\text{O}_3$ ) films were prepared on  $\text{Al}_2\text{O}_3$ -TiC substrates by RF diode sputtering. The target sputtering power was varied from 4 to 8 kW. The effects of target sputtering power on the structure and mechanical properties of alumina films were investigated. The results show that the structure of the alumina films deposited at all the target sputtering powers is amorphous. However, under the exposure to the electron beam during the Transmission Electron Microscopy (TEM) measurements, the structure of alumina films becomes crystalline. The hardness and elastic modulus of alumina films were found to increase as the target sputtering power was increased.

**Keywords:** Alumina Film, Sputtering Power Target, RF Diode Sputtering,  $\text{Al}_2\text{O}_3$ -TiC Substrate

## 1. INTRODUCTION

The deposition of metal oxide films by sputtering technique has been widely used in thin film technology because of its simple method to produce films (Kiyotakawa and Shigeru, 1992). Alumina ( $\text{Al}_2\text{O}_3$ ) film is one of well-known material used in semiconductor devices such as MFIS device, CMOS, MOSFET and magnetic recording head (Qing *et al.*, 2001; Bartzsch *et al.*, 2003; Bahareh *et al.*, 2005). Because of their excellent properties such as low impurities, high dielectric constant compared to  $\text{SiO}_2$  (Kiyotakawa and Shigeru, 1992; Bahareh *et al.*, 2005), high thermal and chemical stable (Tilo *et al.*, 2003), highest hardness among all oxides, insoluble in inorganic acid and fracture resistance (Jochen *et al.*, 1997). Therefore, alumina thin films were used to make base coat and overcoat layer to protect magnetic recording head (Thurn and Cook, 2004). In magnetic recording head fabrication, both reactive and non-reactive PVD sputtering techniques were used to deposit alumina films depend on the required films properties. In addition, the different deposition parameters such as target sputtering power, substrate bias voltage and process pressure have the influence on the

film properties (Bahareh *et al.*, 2005; Thurn and Cook, 2004; Tan *et al.*, 1995).

In this study, alumina films were prepared by RF, a non-reactive sputtering technique in Ar atmosphere because this technique gives compositional consistency, good thickness uniformity and low-cost manufacturing. The alumina films were deposited on  $\text{Al}_2\text{O}_3$ -TiC substrate of magnetic recording head with different target sputtering powers. The structure and mechanical properties such as hardness, elastic modulus and wear resistance of the films were investigated.

## 2. MATERIALS AND METHODS

### 2.1. Films Preparation

Alumina films were prepared by a commercial RF diode sputtering system (Comptech, 2460) with a frequency of 13.56 MHz. The target was a sintered  $\text{Al}_2\text{O}_3$  (99.50% purity) and a size of 17×17 inch<sup>2</sup>. Substrates used were  $\text{Al}_2\text{O}_3$ -TiC wafer with 6-inch diameter. Sputtering gas was Ar (99.99% purity). The substrates were cleaned with 80°C phosphoric acid and 80% concentration and DI water to remove contamination on the substrate surface.

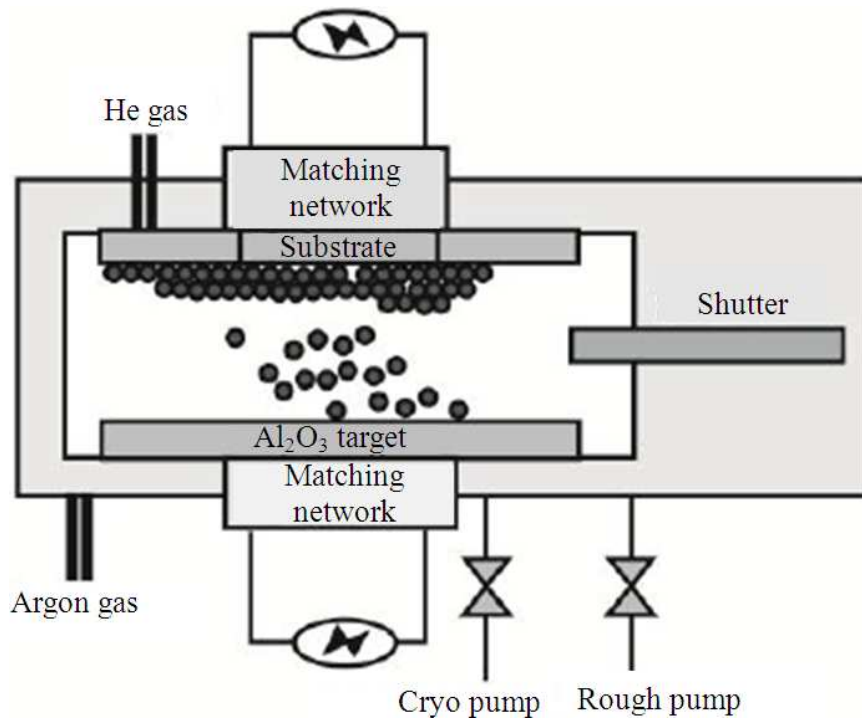


Fig. 1. Schematic of RF diode sputtering system

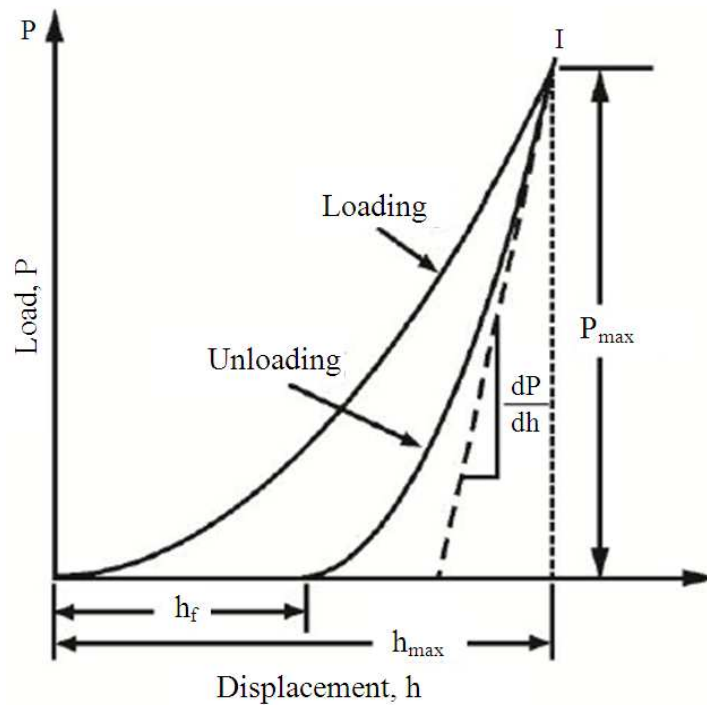


Fig. 2. Schematic of load-displacement curve

The chamber was evacuated to a base pressure of  $2 \times 10^{-6}$  Torr. During sputtering, he gas was used to cool the substrate at the underneath of the substrate for controlling the substrate temperature. Prior to the film deposition, the shutter inside the chamber was closed to separate the substrate and target in order to preclean the substrate and target by sputter etching with Ar plasma. Deposition time was fixed at 22 min for all the prepared films. Details of process parameters for the deposition of  $\text{Al}_2\text{O}_3$  films are shown in **Table 1**.

## 2.2. Characterization

The surface morphology of alumina films was observed by a high resolution scanning electron microscope (SEM: Nova Nano SEM 600). The microstructure of the films was analyzed by a transmission electron microscope (TEM: Tecnai G2 F20 S-Twin). Before TEM analysis the film samples were prepared by focusing ion beam (FIB: Nova Dual Beam, Strata 400s).

The nanoindentation technique was used to measure the hardness of the films. In this study, the nanoindenter (Hysitron, TI 950 Tribonidenter) with a Berkovich diamond indenter, which has a three-sided pyramid geometry, was employed. **Figure 2** shows the typical indentation load-displacement curves measured by nanoindenter.

$P_{\max}$  is a maximum penetration depth of the indenter. The Oliver-Pharr method (Oliver and Pharr, 1992) was used to analyze the load-ing and unloading curves. The hardness is given by the Equation (1):

$$H = \frac{P_{\max}}{A} \quad (1)$$

where, A is the projected contact area which is determined from the value of penetration depth.

The elastic modulus is determined from the slope of the unloading curve at maximum load (i.e.,  $\frac{dP}{dh}$  in **Fig. 1**). Equation (2) shows the elastic modulus as a function of  $\frac{dP}{dh}$  and the projected contact area:

Target sputtering power (kW)	4,5,6,7,8
Substrate bias Voltage (V)	150
Operating pressure (mTorr)	25
Deposition time (min)	22

$$E = \frac{1}{2} \frac{\sqrt{\pi}}{A} \frac{dP}{dh} \quad (2)$$

The slope value can be computed from a linear fit of the upper one-third of the unloading curve. In this study, a test load of 2000  $\mu\text{N}$  was used with a 5 s load time, 2 s hold time and 5 s unload time.

The wear resistance of film was carried out using Hysitron TI950 Triboindenter. The known load (force) was applied on each film at 3 positions to measure wear depth by determining material removal. The applied force used in this study was 20  $\mu\text{N}$  and wear pattern was  $5 \times 5 \mu\text{m}^2$  (HYSITRON, 2002).

## 3. RESULTS AND DISCUSSION

### 3.1. Surface Morphology of Alumina Film

**Figure 3** shows the typical surface morphology of alumina film on  $\text{Al}_2\text{O}_3$ -TiC substrate deposited at a target sputtering power of 7 kW. The defect is observed on all the film surfaces deposited at different target sputtering powers of 4, 5, 6, 7 and 8 kW. Since the alumina film is transparent, the texture of  $\text{Al}_2\text{O}_3$ -TiC grains of the substrate underneath alumina film is also clearly observed.

**Figure 4** shows cross section SEM micrographs of alumina film deposited on of  $\text{Al}_2\text{O}_3$ -TiC substrate at 4 and 7 kW. It is seen that the thickness of alumina film deposited at target sputtering power 7 kW is higher than that of 4 kW. Furthermore, no grains of  $\text{Al}_2\text{O}_3$  appeared in both films, indicating that  $\text{Al}_2\text{O}_3$  films are amorphous. In **Fig. 4**, the black and white areas in the substrate correspond to the  $\text{Al}_2\text{O}_3$  and TiC grains, respectively.

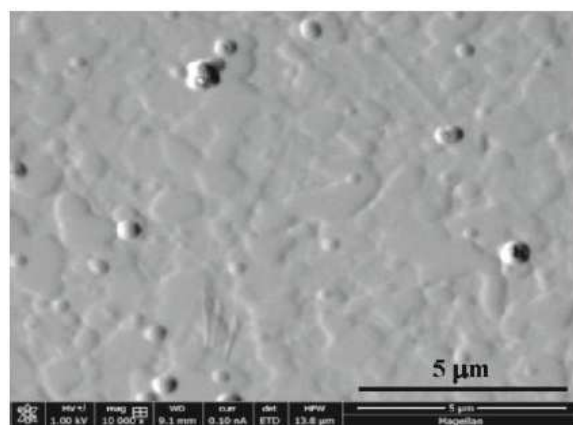


**Fig. 3.** SEM micrograph of alumina film on  $\text{Al}_2\text{O}_3$ -TiC substrate deposited at a sputtering power of 7 kW

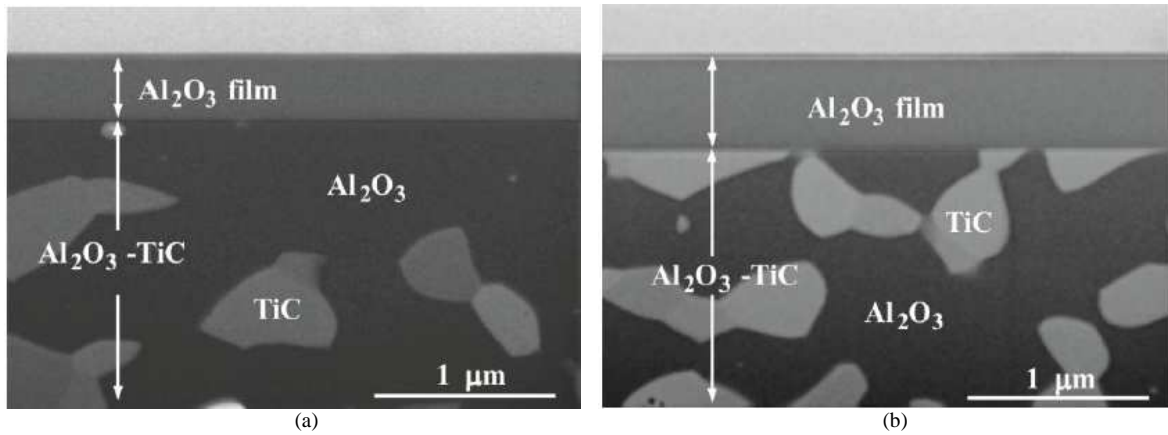


Fig. 4. SEM micrograph of alumina film on Al<sub>2</sub>O<sub>3</sub>-TiC substrate deposited at target sputtering powers of (a) 4 kW and (b) 7 kW

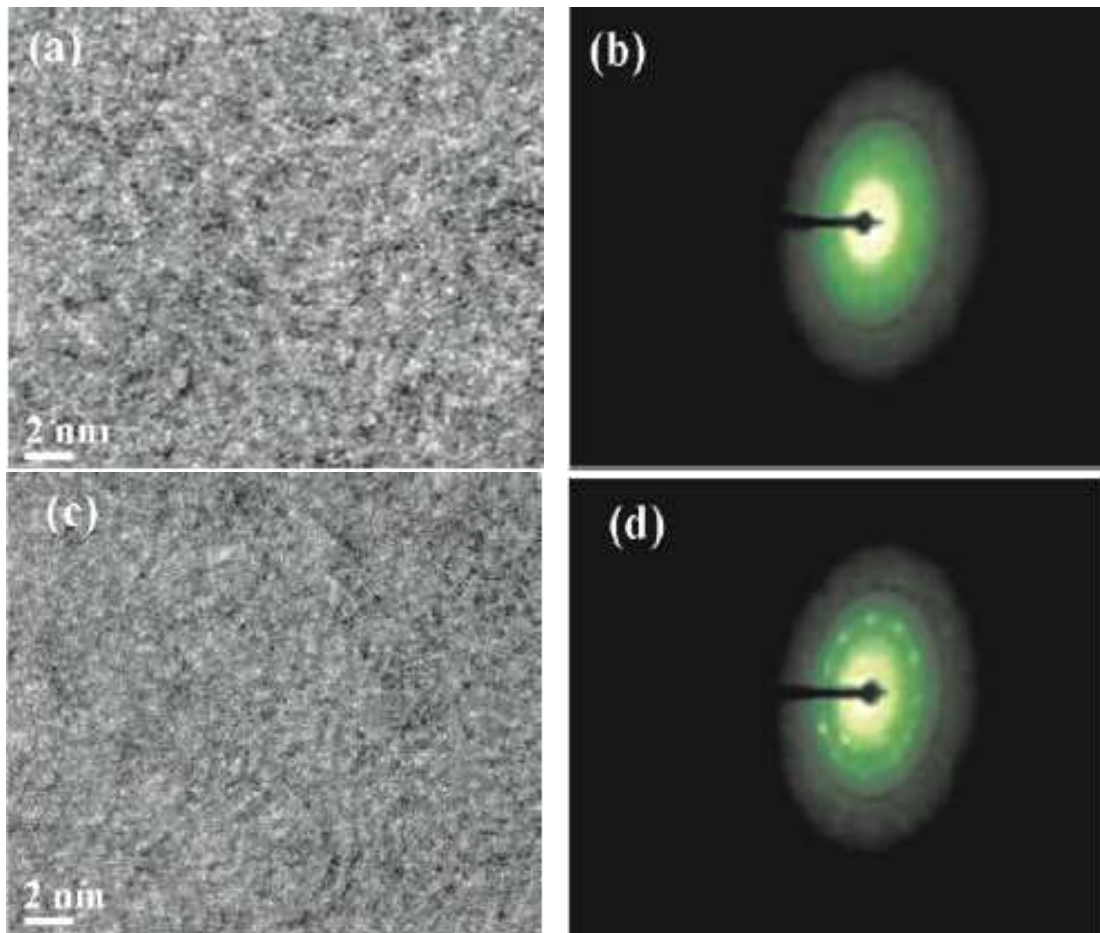


Fig. 5. (a) TEM bright-field image of alumina film on Al<sub>2</sub>O<sub>3</sub>-TiC substrate deposited at a target sputtering power of 7 kW and (b) corresponding SAED patterns, (c) TEM bright-field image of alumina film after 30 sec under electron beam and (d) corresponding SAED patterns

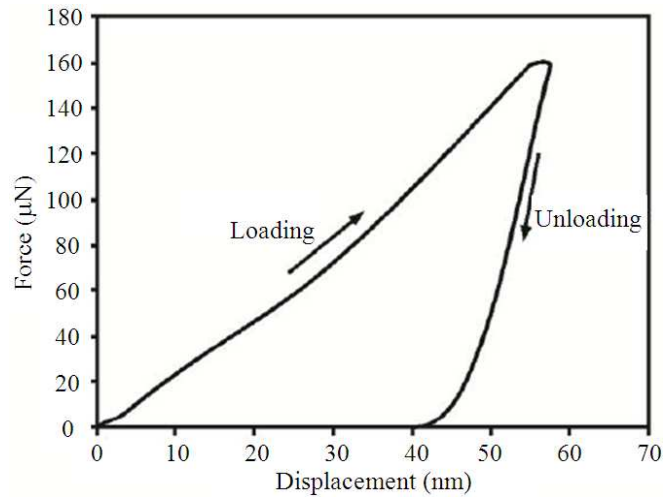


Fig. 6. Typical load-displacement curve of alumina film

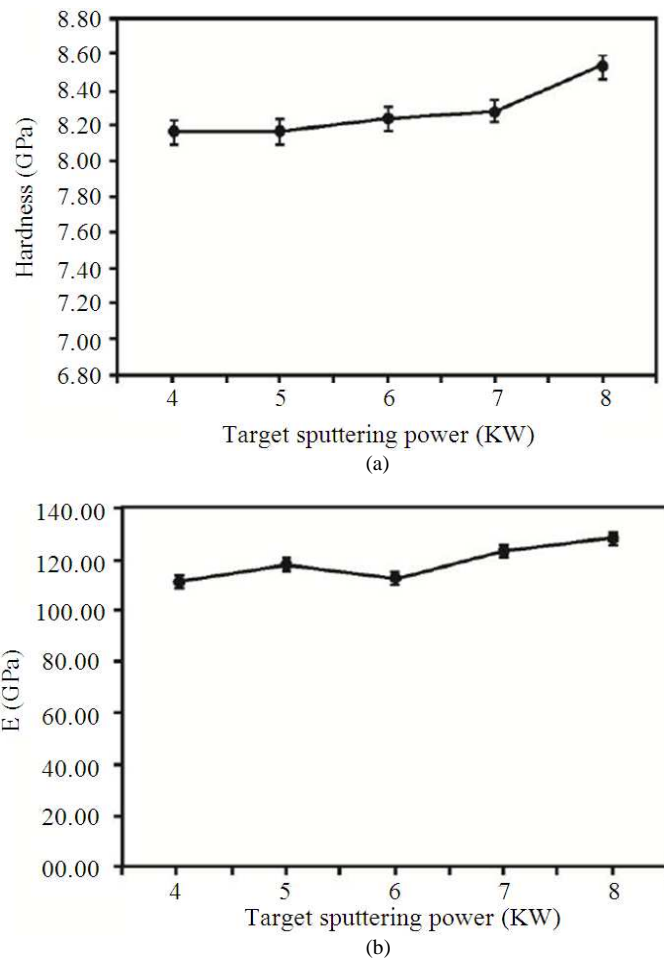
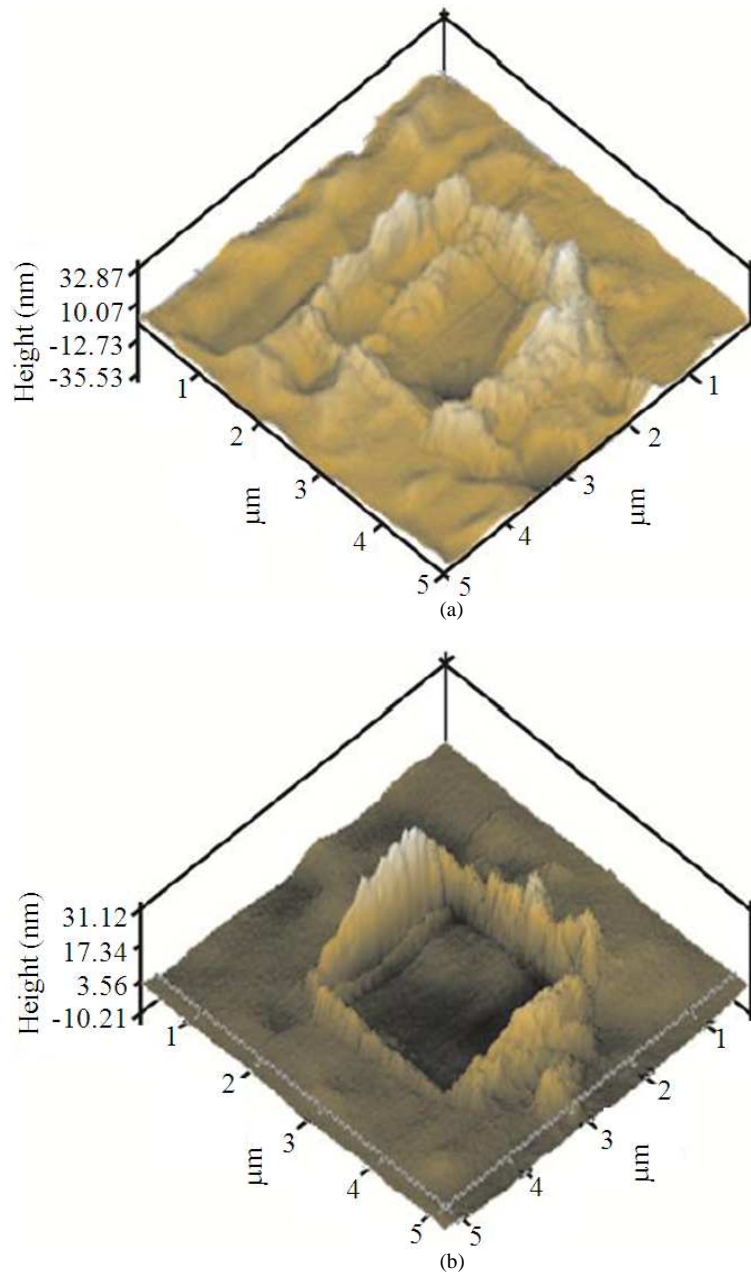


Fig. 7. Variation of (a) hardness and (b) elastic modulus of alumina film as a function of target sputtering power



**Fig. 8.** AFM image of the wear depth of alumina film deposited at target sputtering powers of (a) 4 kW and (b) 7 kW

### 3.2. Microstructure of Alumina Film

**Figure 5(a) and 5(b)** show the initial TEM bright-field image and the corresponding Selected-Area Electron Diffraction (SAED) patterns of alumina film on  $\text{Al}_2\text{O}_3$ -TiC substrate deposited at a sputtering power of 7 kW, respectively. **Figure 5(c) and 5(d)**

show the TEM bright-field image and the corresponding Selected-Area Electron Diffraction (SAED) patterns of alumina film after the alumina film was exposed to electron beam for 30 sec. The electron diffraction patterns in **Fig. 5(b)** shows no spotty rings, indicating that the structure of alumina film is initially amorphous.

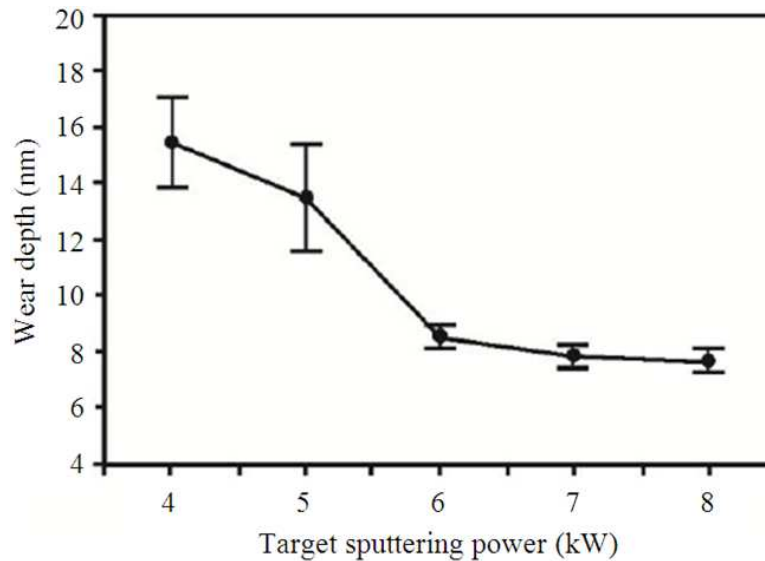


Fig. 9. Variation of wear depth as a function of target sputtering power

However, the spotty rings was clearly observed after the alumina film was exposed to the electron beam for 30 s as shown in Fig. 5(d). This indicates that the alumina film becomes crystalline structure.

### 3.3. Mechanical Properties of Alumina Film

Figure 6 shows the typical load-displacement curve of alumina film on  $\text{Al}_2\text{O}_3$ -TiC substrate deposited at a target sputtering power of 7 kW. The hardness and elastic modulus were then determined.

Figure 7 shows the values of hardness and elastic modulus as a function of target sputtering powers. It was found that the hardness and elastic modulus values increased from 8.16 to 8.54 GPa and 111.2 to 127.6 GPa, respectively, as the target sputtering power was increased from 4 to 8 kW. The results are in good agreement with those reported in literature (Chou *et al.*, 1991).

Figure 8 shows the AFM image of the wear depth on the alumina film deposited at sputtering powers of 4 and 7 kW, respectively. The wear depth value as a function of target sputtering power is shown in Fig. 9. It is seen that the wear depth value decreased from 15.58 to 7.98 nm as the target sputtering power was increased from 4 to 8 kW. This is due to the increase in the film hardness with increasing target sputtering power.

## 4. CONCLUSION

We investigated the effects of target sputtering power on the structure and mechanical properties of

alumina film on  $\text{Al}_2\text{O}_3$ -TiC substrate as deposited by RF diode sputtering technique. The results show that the structure of the alumina films deposited at all the target sputtering powers is amorphous. However, under the exposure to the electron beam during the Transmission Electron Microscopy (TEM) measurements, the structure of alumina films becomes crystalline. In addition, it was found that the hardness and elastic modulus of alumina films increased with increasing target sputtering power. The wear-resistance test correspond to the wear depth shows that the wear depth value decreased with increasing target sputtering power. The wear depth results are in agreement with those of hardness values. This studied reveal that alumina film prepared by RF diode sputtering under optimized condition exhibit good mechanical properties which makes film suitable for magnetic recording head application.

## 5. ACKNOWLEDGEMENT

This study was supported by NECTEC and magnetic head division of Western digital Ltd.

## 6. REFERENCES

- Bahareh, B., Y. Yizhang and A. Mehdi, 2005. Thermal property measurement of thin aluminum oxide layers for Giant Magnetoresistive (GMR) head applications. *Int. J. Heat Mass Trans.*, 48: 2023-2031. DOI: 10.1016/j.ijheatmasstransfer.2004.12.010

- Bartzsch, H., P. Frach and K. Goedicke, 2003. Properties of SiO<sub>2</sub> and Al<sub>2</sub>O<sub>3</sub> films for electrical insulation applications deposited by reactive pulse magnetron sputtering. *Surface Coat. Technol.*, 174-175: 774-778. DOI: 10.1016/S0257-8972(03)00384-0
- Chou, T.C., T.G. Nieh, S.D. McAdara and G.M. Pharr, 1991. Microstructures and mechanical properties of thin films of aluminum oxide. *Scripta Metallurgica*, 25: 2203-2208.
- HYSITRON, 2002. Scanning wear-measuring wear resistance at the Nanoscale.
- Jochen, M., D. William and M. Allan, 1997. Phase formation and mechanical properties of alumina coatings prepared at substrate temperatures less than 500°C by ionized and conventional sputtering. *Surface Coat. Technol.*, 94-95: 179-183. DOI: 10.1016/S0257-8972(97)00437-4
- Kiyotakawa, W. and H. Shigeru, 1992. *Handbook of Sputter Deposition Technology: Principles, Technology and Applications*. Noyes Publications, New Jersey, ISBN-10: 0815512805, pp: 304.
- Tan, M. S.I. Tan and Y. Shen, 1995. Ion beam deposition of alumina for recording head applications. *IEEE Trans. Magnet.*, 31: 2694-2696. DOI: 10.1109/20.490095
- Oliver, W.C. and G.P. Pharr, 1992. An improved technique for determining hardness and elastic modulus using load and displacement sensing indentation experiments. *J. Mater. Res.*, 7: 1564-1583. DOI: 10.1557/JMR.1992.1564
- Qing, W., Z. Ninglin, W. Lianwei, S. Qinwo and L. Chenglu, 2001. Preparation of high quality amorphous Al<sub>2</sub>O<sub>3</sub> thin film on silicon and its applications. *Proceedings of the 6th International Conference on Solid-State and Integrated-Circuit Technology*, Oct. 22-25, IEEE Xplore Press, pp: 1468-1470. DOI: 10.1109/ICSICT.2001.982181
- Thurn, J. and R.F. Cook, 2004. Mechanical and thermal properties of physical vapour deposited alumina films Part I Thermal stability. *J. Mater. Sci.*, 39: 4799-4807. DOI: 10.1023/B:JMSC.0000035318.95497.d1
- Tilo, P., N. Thomas and N. Andreas, 2003. The properties of aluminum oxide and nitride films prepared by d.c. sputter-deposition from metallic targets. *Surface Coat. Technol.*, 163-164: 164-168. DOI: 10.1016/S0257-8972(02)00484